MAGNETIC AND MICROWAVE ABSORPTION CHARACTERISTICS OF Ti^{2+}-Mn^{4+} SUBSTITUTED BARIUM HEXAFERRITE

Azwar Manaf[1*], Mas Ayu Elita Hafizah[1], Belyamin[2], Benhur Nainggolan[2], Maykel Manawan[1,2]

[1]*Postgraduate Program of Materials Science Study, Faculty of Mathematics and Natural Sciences, Universitas Indonesia, Kampus UI Depok, Depok 16424, Indonesia*
[2]*Energy Engineering, Jakarta State of Polytechnic, Depok 16424, Indonesia*

ABSTRACT

Series of Ti^{2+}-Mn^{4+} ions substituted $BaFe_{12-2x}Ti_xMn_xO_{19}$ samples with x = 0.0–0.8 have been studied to find out the effect of ion substitution on their microstructure, magnetic, and microwave absorption characteristics. The materials were synthesized through the mechanical alloying process. X-ray diffraction pattern for all sintered samples confirmed that the materials are single phase materials with $BaFe_{12}O_{19}$ structure. Referring to the results, it is shown that all samples that are subject to ultrasonic irradiation treatment characterized by a crystallite size distribution with the width get slimmer and mean crystallite size get smaller as the substitution level increased from x = 0 to x = 0.8. A sample of latter composition has fine crystals between 10–200 nm with the mean size of 42 nm. The effect of ionic substitution also affected the magnetic properties in which coercivity decreased proportionally with an increase of x value. The saturation magnetization increased to 0.41 T at x = 0.4, and then decreased for higher x values. Hence, the increase occurred only in samples with low-level substitutions of Ti^{2+}-Mn^{4+} ions. Microwave absorption characterization clearly shows that the reflection loss (RL) value of Ti^{2+}-Mn^{4+} substituted $BaFe_{12-2x}Ti_xMn_xO_{19}$ samples was enhanced from 2.5 dB in a doped free sample (x = 0) to 22 dB (~92% absorption) in a sample with x = 0.6 in the frequency range 8–12 GHz.

Keywords: Barium hexaferrite; Magnetic properties; Mechanical alloying; Radar absorbing materials; Reflection loss

1.   INTRODUCTION

The utilization of devices which operate in a wide range of frequencies, including in gigahertz, has increased recently. This might bring some consequences to the devices like information and communication that used electronics components due to electromagnetic interference (EMI) effects. Hence, the use of microwave absorbing materials would be one of the promising ways to suppress EMI (Naito & Suetake, 1971). Many reports have shown that ferrites and metallic magnetic materials can be used as conventional microwave absorbing materials. The spinel-type ferrites, which are known widely as soft magnets, should also be suitable for electromagnetic waves (EM) absorption because ferrites ceramic based materials possess a relatively high magnetization value. However, most of the spinel ferrites have a limit in the working frequencies in which the materials can only be utilized in low frequencies. Other materials like metal based magnets, which show high permeability and magnetization values,

would also be suitable candidates for EM absorbers, but they have to be insulated to prevent an eddy current (Yoshida et al., 1999). Some reports have shown that the most suitable material for EM absorbers is barium hexaferrites (BHF). BHF has a high saturation magnetization, high Curie temperature, high resistance and chemical stablility, and has been used as low-cost permanent magnet applications. However, BHF has a high value of uniaxial anisotropy field and magnetic permeability. Consequently, its resonant absorption frequency of $f_0 = 42.5$ GHz is very high (Pullar, 2012).

In order to employ BHF as microwave absorbing materials, many studies have focused on modifying its magnetic property, mainly the magnetocrystalline anisotropy constant, by substituting Fe^{3+} ions with divalent, trivalent, and tetravalent cations or cation combination (Pullar, 2012). Sample preparation could be performed using one of the following methods: sol–gel (Han et al., 2009), mechano-combustion (Ataie & Zojaji, 2007), ammonium nitrate melts (Topal et al., 2007), citrate–nitrate gel combustion (Chaudhury et al., 2008), co-precipitation (Moghaddam & Ataie, 2006) and mechanical alloying (Mendoza-Suarez et al., 2001). Those methods were widely adopted by many researchers because the method is easy to implement on both small and large scales (Wang et al., 2000).

Most of the ionic substitutions for Fe in BHF have been reported to decrease the total magnetization value followed by a decrease in their corresponding coercivities. Substituting ions like La^{3+} (Seifert et al., 2009), Mn^{3+} (Lee et al., 2009), Co^{2+}-Zr^{4+} (Lia & Chen, 2002), Ti^{4+}-Mn^{4+} (Turilli et al., 1986; Repi et al., 2014) and many other combinations have been shown effective in improving EM absorption characteristics of ionic substituted BHF. In other reports, like the works of Bsoul et al. (2010) on Ti^{2+}-Ru^{4+} and Liu et al. (2001) on Co^{2+}-Mn^{2+}-$2Sn^{4+}$, an increase in total magnetization of BHF was obtained. In this study, in order to meet requirements for a good microwave absorption material in the X band frequency range (8−12.4 GHz), Fe ion in BHF was replaced partially with Ti^{2+}-Mn^{4+} ions.

2.   EXPERIMENTAL PROCEDURE

Samples of $BaFe_{12-2x}Ti_xMn_xO_{19}$ with $x = 0$, 0.2, 0.4, 0.6, and 0.8 were prepared through mechanical alloying and solid state reaction technique. Stoichiometry quantities of analytical-grade $BaCO_3$, Fe_2O_3, TiO and MnO_2 precursors with a purity of greater than 99% were mixed and milled using a planetary ball mill with steel balls to a powder:weight ratio of 10:1. Powders obtained after 20 hours of milling time were pelletized and sintered at a temperature of 1100^oC for 2 hours to obtain crystalline samples. The sintered samples were crushed and re-milled in a planetary ball mill for 20 hours, followed by cleaning in a low concentration of chloric acid containing liquid to dissolve excess iron oxides raised from steel vial and balls. The size of milled powders was further reduced by means a power ultrasonicator (Qsonica 700). The X-Ray Diffraction (XRD) of sintered samples was performed using Philips PW3710 diffractometer with Co-K_α radiation. The grain morphology was characterized using an FEI-F50 Scanning Electron Microscope (SEM). The *M-H* loops were measured in applied fields of 0–2000 kA/m at room temperature using Permagraph-L magnetometer. The microwave measurement was conducted on ADVANTEST R3770 Vector Network Analyzer. Data of XRD for all samples were further refined using a structural analysis software for qualitative and quantitative analysis of the diffraction patterns.

Saturation magnetization (M_s) and anisotropy field (H_a) were deduced from numerical analysis of the magnetization curves based on the Law of Approach Saturation, LAS (Grössinger, 1982):

$$M(H) \approx M_s \left(1 - \frac{A}{H} - \frac{B}{H^2} ... \right) + \chi_d H \tag{1}$$

where *M(H)* is the specific magnetization at magnetic field strength *H*, χ_d is the highest field susceptibility, $\frac{A}{H}$ term is related to the existence of inhomogeneity and theoretically, should vanish at high fields, and $\frac{B}{H^2}$ term is related to magnetocrystalline. The region to validate the LAS is determined by the tangent to reduce magnetization M/M_s as the function of reduced field H/H_a.

Microwave absorption properties were evaluated by reflection loss (*RL*), which is derived from the following formula:

$$RL = 20\ log \left| \frac{Z_{in} - Z_0}{Z_{in} + Z_0} \right| \qquad (2)$$

where Z_{in} and Z_o are the input impedance of the EM and the composite medium respectivelly.

3.   RESULTS AND DISCUSSION

3.1.   Phases and Microstructure Analysis

The x-ray diffraction pattern of sintered samples for $BaFe_{12-2x}Ti_xMn_xO_{19}$ compositions with x = 0.0–0.8 has been previously reported (Manawan et al., 2014), of which all diffracted peaks appear in the same 2θ diffraction angle position. Nevertheless, there is a small shift in the diffracted peak positions due to partial replacement of Fe^{3+} ions with Ti^{2+} and Mn^{4+} ions.
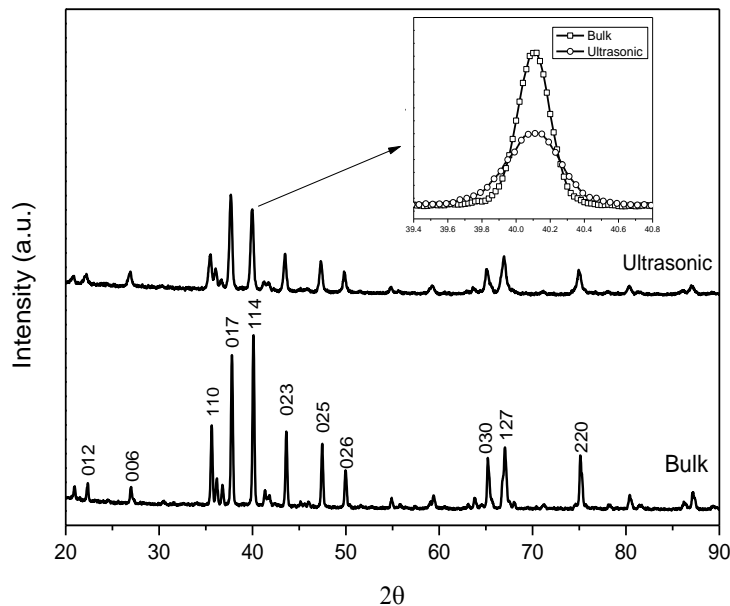

Figure 1 The X-ray diffraction pattern of doped free bulk sample compared with
ultrasonically irradiated sample

Phase analysis of the XRD data has resulted in the conclusion that single phases of Ti^{2+}-Mn^{4+} ions substituted $BaFe_{12-2x}Ti_xMn_xO_{19}$ samples were successfully synthesized. We continue to explore further the microstructure of sample series when samples undergo ultrasonic irradiation in a high power sonicator. Figure 1 compares the x-ray diffraction pattern of x = 0 samples before and after ultrasonic treatment. All ultrasonically treated samples have a similar diffraction pattern characterized by broadening diffraction peaks as shown in the inset of Figure 1. It indicates fine crystallites of the sample. In most cases, the width of diffraction peaks is often used to estimate the mean crystallite size through the Debye-Scherrer equation (Cullity,

1976). However, we analyzed the crystallite size distribution of each sample through refining the XRD data using a PM2K software based on the Whole Powder Pattern Modelling (WPPM) method (Scardi & Leoni, 2002). Compilation of the results of the analysis is shown in Figure 2a, followed by SEM micrographs for each sample showing the crystallites in the sample (Figures 2b–2f). Figure 2a clearly indicates that a progressive reduction in crystallite size has taken place in crystalline particles which experienced ultrasonic treatments, as more Fe^{3+}ions in $BaFe_{12}O_{19}$ are replaced with $Ti^{2+}$and Mn^{4+}ions. Sample with x = 0, characterized by a broader crystallite size distribution in the range about10-800 nm with the mean size 209 nm, showed both the width of the distribution and mean crystallite size was brought down further to be more slim and small, respectively, as the substitution level was increased from x = 0 to x = 0.8. In the latter composition, the sample has a crystallite size between 10 nm and 200 nm with the mean size of 42 nm. The crystallites of ultrasonically treated samples can be seen in Figure 2b, which shows high resolution SEM micrographs of each treated sample. The micrographs showed that most of the crystals are bound together into larger particles due to strong cohesive force among fine crystals.

In our previous work (Manaf & Hafizah, 2012), we employed a similar method to refine the crystallite size of mechanically alloyed crystalline particles through ultrasonic irradiation in the liquid media containing particles.
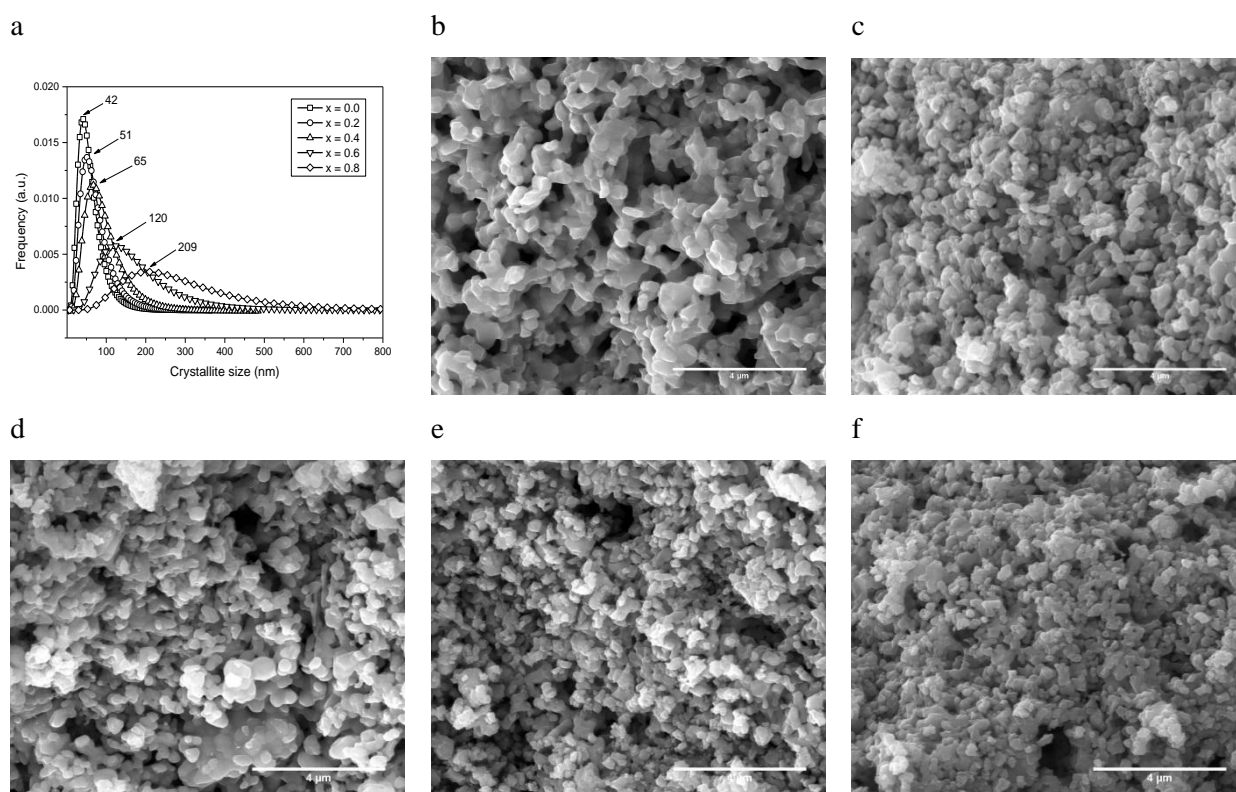

Figure 2 (a) The crystallite size distribution; and (b-f) SEM Micrographs showing crystallite size reduction of $BaFe_{12-2x}Ti_xMn_xO_{19}$samples after ultrasonic irradiation for 5 hours

It was shown that fragmented crystallites were achieved by the destruction of particles and crystallites through the creation of thousands of cavitation bubbles, which eventually resulted in an implosive collapse accompanied by local sound waves with pressures of hundreds of atmospheres (Gedanken, 2004). The shock waves generated by the implosive collapse of bubbles in liquids containing particles drive the particles together at extremely high speeds, causing a series of unavoidable collisions among the particles (Prozorov et al., 2004), resulting

in crystallites fragmentation. The crystallite size distribution and SEM micrograph of $BaFe_{12-2x}Ti_xMn_xO19$ (x = 0.0–0.8) samples as seen in Figure 2 confirmed once again that the fragmentation of large crystals is possible by a high power ultrasonic irradiation leading to a slim crystallite size distribution with a small mean crystallite size. The SEM micrographs of samples also indicate that the more fraction of Ti^{2+} and Mn^{4+} ions substituted the Fe^{3+} ions in BHF, the more refine crystallite sizes were obtained in the sample. This suggests that the ions substituted BHF samples must be more brittle than that of the doped free sample.

3.2. Magnetic and Microwave Characteristics

The hysteresis loop of $BaFe_{12-2x}Ti_xMn_xO_{19}$ samples (x = 0.0–0.8) has been reported previously (Manawan et al., 2014). In Figure 3, their respective calculated values of total polarization (J_s), the anisotropy field (H_a) and measured values of coercivity (H_c) are plotted. This is done in order to find out the effect of Ti^{2+} and Mn^{4+} ion substitution in the magnetic properties of $BaFe_{12-2x}Ti_xMn_xO_{19}$ samples (x = 0.0–0.8). For the sample with x = 0, which is the un-doped BHF, the coercivity (H_c) and total polarization (J_s) were found to be 282.5 kA/m and 0.38 T, respectively. Such values are typical magnetic properties of BHF permanent magnets. The plot of coercivity, H_c in Figure 3 also indicates that (H_c) of doped samples decreases with increasing x.
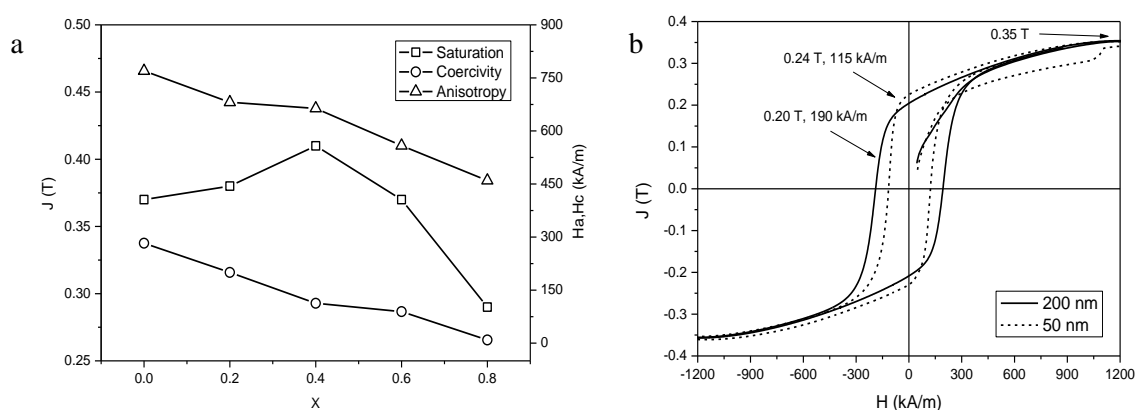

Figure 3 (a) Calculated J_s, H_a and measured H_c of $BaFe_{12-2x}Ti_xMn_xO_{19}$; (b) *J-H* loops of nanocrystalline $BaFe_{12}O_{19}$ samples

Although the coercivity of permanent magnets is microstructure-sensitive, especially in microcrystalline samples in which the grains are relatively large, the magnetic domains can form in the grains. However, a decrease in coercivity in doped samples is more likely caused by a change in a magnetocrystalline anisotropy constant (K) of their respective magnetic phase. This can be seen in the plot of calculating anisotropy field, H_a of $BaFe_{12-2x}Ti_xMn_xO_{19}$ samples in Figure 3, showing a continued decrease in H_a value with increasing x. The H_a decreased almost linearly with x due to a change in the magnetocrystalline constant. According to the LSA calculation, we obtained a K value for x = 0 is $2.67\times10^5 J/m^3$, which was not much different from the published K = $3.3\times10^5 J/m^3$ for the BHF (Rezlescu et al., 1999). The K value of doped samples decreased as x increased. For x = 0.8, the K value was $1.16\times10^5 J/m^3$, only double that of α-Fe ($0.46\times10^5 J/m^3$) (Fischer et al., 1998). This explains why the coercivity of a sample with x = 0.8 is very low, about 9.18 kA/m, which indicates that the sample becomes a soft magnet. Another factor responsible for the decrease in coercivity is the extrinsic effect caused by the extremely fine crystallite size. The mean crystallite size of all samples is below 210 nm, which much smaller than the size of single domain particle (460 nm) for the BHF (Rezlescu et al., 1999). With such fine crystallite size, grain exchange interaction effect (Manaf et al., 1993) might be responsible for the decrease in coercivity of the samples. In the current

case, the effect is demonstrated in Figure 3b, in which the hysteresis loop of a BHF sample of 200 nm mean crystallite size is compared with that of 50 nm. The latter sample shows an enhancement in remanence magnetization above the theoretical value based on the Stoner-Wohlfarth theory (Stoner & Wohlfarth, 1948), but with a decrease in coercivity due to grain exchange interaction effect.
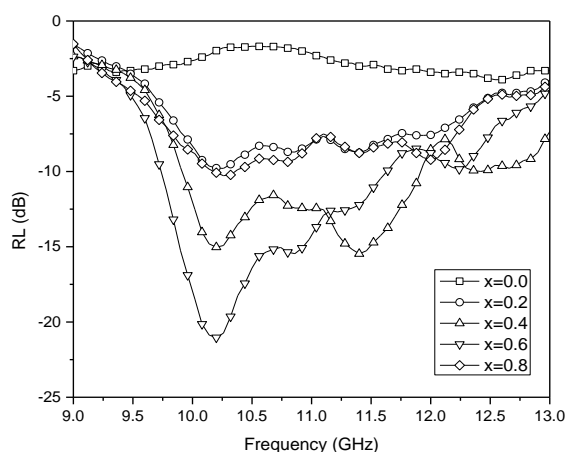

Figure 4 Reflection loss of $BaFe_{12-2x}Ti_xMn_xO_{19}$ samples

Figure 4 shows the reflection loss (RL) value of $BaFe_{12-2x}Ti_xMn_xO_{19}$ samples in the frequency range 8–12.4 GHz. For the doped-free BHF sample (x = 0), the RL value in the whole range is only about -2.5 dB, which is very low when compared with those of doped BHF samples. The reason for almost no absorptions in the frequency range for a sample with x = 0 might be due to a high ferromagnetic resonance frequency of 42.5 GHz possessed by the sample (Pullar, 2012). The sample also possesses the largest anisotropy field and coercivity values when compared with the doped samples. Nevertheless, the RL improved significantly in the frequency range of all doped samples (x > 0) as indicated by the results in Figure 4, which show the absorption of EM wave increased with increasing x, except for the sample with the largest x value (0.8), where the RL returned to near identical with x = 0.2 sample. When referring to the magnetic properties in Figure 3, a sample with x = 0.8 has a very low coercivity of 9.2 kA/m and a very low total magnetization of only 0.29 T, the lowest value among the doped samples. On the other hand, the samples with x = 0.4 and 0.6 have total magnetization values of 0.41 T and 0.37 T, respectively, with respective coercivity of 112.7 kA/m and 89.11 kA/m. However, comparison of the RL values among the doped samples shows that the RL value for x = 0.6 and 0.4 are nearly identical to each other and much higher than those those of x = 0.2 and 0.8. The maximum absorption peaks with RL = 22 dB (~92%) at frequency of ~10.2 GHz obtained in a doped sample with x = 0.6. Based on the results as shown in Figure 3 and Figure 4, we can take the conclusion that sample with a high RL value requires high total magnetization and low coercivity values. Materials with a high total magnetization and low magnetocrystalline anisotropy constant values would be potential candidates for microwave absorbing materials (MAM) applications.

4. CONCLUSION

This study has demonstrated that the substitution of Ti^{2+} and Mn^{4+} ions in $BaFe_{12-2x}Ti_xMn_xO_{19}$ materials with x = 0.2–0.8 makes a considerable change in extrinsic properties in terms of crystallite sizes, magnetic properties, and microwave characterization. All synthesized materials are a nanocrystalline material with the mean crystallite size below 210 nm. The substitution of Fe^{3+} cations with Ti^{2+}-Mn^{4+} changed the magnetocrystalline anisotropy constant of x = 0 from

2.67×10^5 J/m^3 down to 1.16×10^5 J/m^3 at x = 0.8. The change decreased the coercivity value for the whole range of substitution. The large value of RL in $BaFe_{12-2x}Ti_xMn_xO_{19}$ samples requires magnetic properties with high remanence and low coercivity values. It was shown that about 95% intensity of the incoming EM waves can be absorbed in a doped sample with x = 0.6 composition.

5.   ACKNOWLEDGEMENT

6.   REFERENCES

Ataie, A., Zojaji, S.E., 2007. Synthesis of Barium Hexaferrite Nano-particles via Mechano-combustion Route. *Journal of Alloys and Compounds,* Volume 431(1–2), pp. 331–336

Bsoul, I., Mahmood, S., Lehlooh, A.F., 2010. Structural and Magnetic Properties of $BaFe_{12-2x}Ti_xRu_xO_{19}$. *Journal of Alloys and Compounds,* Volume 498, pp. 157–161

Chaudhury, S., Rakshit, S., Parida, S., Singh, Z., Mudher, K.S., Venugopal, V., 2008. Studies on Structural and Thermo-chemical Behavior of $MFe_{12}O_{19}(s)$ (M = Sr, Ba and Pb) Prepared by Citrate–nitrate Gel Combustion Method. *Journal of Alloys and Compounds,* Volume 455(1–2), pp 25–30

Cullity, B.D., 1976. *Elements of X-ray Diffraction*. Addison-Wesley Publishing Co. Inc., Reading

Fischer, R., Leineweber, T., Kronmuller, H., 1998. Fundamental Magnetization Processes in Nanoscaled Composite Permanent Magnets. *Physical Review B,* Volume 57, 10723

Gedanken, A., 2004. Using Sonochemistry for the Fabrication of Nanomaterials. *Ultrasonics Sonochemistry,* Volume 11, pp. 47–55

Grössinger, R., 1982. Correlation between the Inhomogeneity and the Magnetic Anisotropy in Polycrystalline Ferromagnetic Materials. *Journal of Magnetism and Magnetic Materials,* Volume 28(1–2), pp. 137–142

Han, M., Ou, Y., Chen, W., Deng, L., 2009. Magnetic Properties of Ba-M-type Hexagonal Ferrites Prepared by the Sol–gel Method with and without Polyethylene Glycol Added. *Journal of Alloys and Compounds,* Volume 474(1–2), pp. 185–189

Lee, I.K., Sur, J.C., Shim, I.-B., Kim, A.C., 2009. The Effect of Manganese Substituted M-type Hexagonal Ba-ferrite. *Journal of Magnetics,* Volume 14, pp. 93–96

Lia, Z.W., Chen, L., 2002,. Studies of Static and High-frequency Magnetic Properties for M-type Ferrite $BaFe_{(12-2x)}Co_xZr_xO_{19}$. *Journal of Applied Physics,* Volume 92, pp. 3902–3907

Liu, Y., Drew, M.G., Liu, Y., 2001. Preparation and Magnetic Properties of Barium Ferrites Substituted with Manganese, Cobalt and Tin. *Journal of Magnetism and Magnetic Materials,* Volume 323, pp. 945–953

Manaf, A., Buckley, R.A., Davies, H.A., 1993. New Nanocrystalline High-remanence Nd-Fe-B Alloys by Rapid Solidification. *Journal of Magnetism and Magnetic Materials*, Volume 128(3), pp. 302–306

Manaf, A., Hafizah, E., 2012. Particle Size of Mechanically Alloyed $La_{0.5}Sr_{0.5}Fe_{0.5}Mn_{0.25}Ti_{0.25}O_3$ Powders Prepared with the Assistance of Ultrasonic Irradiation. *Journal of Materials Science Research*, Volume 1(4), pp. 98–105

Manawan, M., Manaf, A., Soegijono, B., Yudi, A., 2014. Microstructural and Magnetic Properties of Ti^{2+}-Mn^{4+} Substituted Barium Hexaferrite. *Advanced Materials Research,* Volume 896, pp. 401–405

Mendoza-Suárez, G., Matutes-Aquino, J., Escalante-García, J., Mancha-Molinar, H., Ríos-Jara, D., Johal, K., 2001. Magnetic Properties and Microstructure of Ba-ferrite Powders Prepared by Ball Milling. *Journal of Magnetism and Magnetic Materials,* Volume 223(1), pp. 55–62

Moghaddam, K.S., Ataie, A., 2006. Role of Intermediate Milling in the Processing of Nano-size Particles of Barium Hexaferrite via Co-precipitation Method. *Journal of Alloys and Compounds,* Volume 426(1–2), pp. 415–419

Naito, Y., Suetake, K., 1971. Application of Ferrite to Electromagnetic Wave Absorber and its Characteristics. *IEEE Transactions on Microwave Theory and Techniques,* Volume 19(1), pp. 65–72

Prozorov, T., Prozorov, R., Suslick, K.S., 2004. High Velocity Interparticle Collisions Driven by Ultrasound. *Journal of American Chemical Society,* Volume 126, pp. 13890–13891

Pullar, R.C., 2012. Hexagonal Ferrites: A Review of the Synthesis, Properties and Applications of Hexaferrite Ceramics. *Progress in Materials Science,* Volume 57, pp. 1191–1334

Repi, V., Manaf, A., Soegijono, B., 2014. Magnetic Properties and Reflection Loss Characteristic of Mn-Ti Substituted Barium-Strontium Hexaferrite. *Advanced Materials Research,* Volume 896, pp. 418–422

Rezlescu, L., Rezlescu, E., Popa, P.D., Rezlescu. N., 1999. Fine Barium Hexaferrite Powder Prepared by the Crystallisation of Glas. *Journal of Magnetism and Magnetic Materials,* Volume 193, pp. 288–290

Scardi, P., Leoni, M., 2002. Whole Powder Pattern Modelling. *Acta crystallographica. Section A, Foundations of crystallography,* Volume 58(Pt 2), pp. 190–200

Seifert, D., Topfer, J., Langenhorst, F., LeBreton, J.M., Chiron, H., Lechevallier, L., 2009. Synthesis and Magnetic Properties of La-substituted M-type Sr Hexaferrites. *Journal of Magnetism and Magnetic Materials,* Volume 321, pp. 4045–4051

Stoner, E.C., Wohlfarth, E.P., 1948. A Mechanism of Magnetic Hysteresis in Heterogeneous Alloys. *Philosophical Transactions of the Royal Society*, Volume A–240, pp. 599–642

Topal, U., Ozkan, H., Dorosinskii, L., 2007. Finding Optimal Fe/Ba Ratio to Obtain Single Phase $BaFe_{12}O_{19}$ Prepared by Ammonium Nitrate Melt Technique. *Journal of Alloys and Compounds,* Volume 428, pp. 17–21

Turilli, G., Licci, F., Rinaldi, S., 1986. Mn^{2+}, Ti^{4+} Substituted Barium Ferrite. *Journal of Magnetism and Magnetic,* Volume 59(1–2), pp. 127–131

Wang, S., Ding, J., Shi, Y., Chen, Y., 2000. High Coercivity in Mechanically Alloyed $BaFe_{10}Al_{2}O_{19}$. *Journal of Magnetism and Magnetic Materials,* Volume 219(2), pp. 206–212

Yoshida, S., Sato, M.E., Sugiwara, Y.S., 1999. Permeability and Electromagnetic-interference Characteristics of Fe-Si-Al Alloy Flakes Polymer Composite. *Journal of Applied Physics,* Volume 85(8), pp. 4636–4638